On the use of hydrodynamic modelling and random forest classifiers for the prediction of hypoxia in coastal lagoons

Science of the Total Environment 951 (2024) 175424

Contents lists available at ScienceDirect

Science of the Total Environment

journal homepage: www.elsevier.com/locate/scitotenv

On the use of hydrodynamic modelling and random forest classifiers for the prediction of hypoxia in coastal lagoons

Irene Simonetti *, Claudio Lubello, Lorenzo Cappietti

Dept. of Civil and Environmental Engineering, University of Florence, Italy

HIGHLIGHTS

- Prediction and forecast of dissolved oxygen (DO) in anthropized, eutrophic coastal lagoons
- Synergic use of hydrodynamic modelling, measurements and Random Forest algorithms
- SHapley Additive exPlanations is applied to interpret the prediction of the Random Forest models.
- The method can capture the spatial heterogeneity of DO in the lagoon, with high resolution in time.
- Accuracy of 90 % in forecasting DO levels and detecting hypoxia up to 10 days in advance

GRAPHICAL ABSTRACT

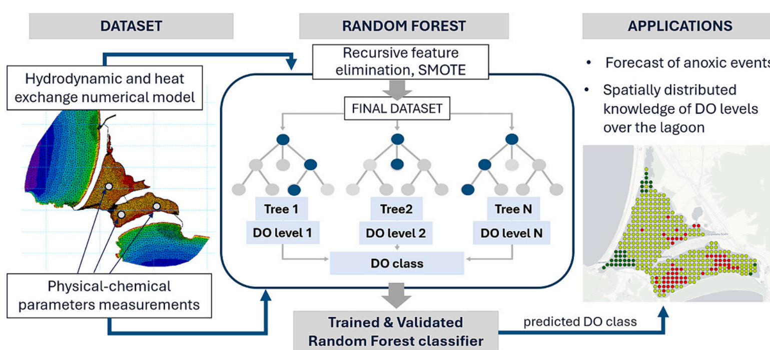

ARTICLE INFO

Editor: Fernando Pacheco

Keywords:
Hypoxia
Random Forest
Forecast
Dissolved oxygen
Eutrophic lagoon
Hydrodynamics modelling

ABSTRACT

Hypoxia is one of the fundamental threats to water quality globally, particularly for partially enclosed basins with limited water renewal, such as coastal lagoons. This work proposes the combined use of a machine learning technique, field observations, and data derived from a hydrodynamic and heat exchange numerical model to predict, and forecast up to 10 days in advance, the occurrence of hypoxia in a eutrophic coastal lagoon. The random forest machine learning algorithm is used, training and validating a set of models to classify dissolved oxygen levels in the lagoon. The Orbetello lagoon, in the central Mediterranean Sea (Italy), has provided a test case for assessing the reliability of the proposed methodology. Results proved that the methodology is effective in providing a reliable short-term evaluation of DO levels, with a high resolution in both time and space throughout an entire lagoon. An overall classification accuracy of up to 91 % was found in the models, with a score for identifying the occurrence of severe hypoxia - i.e. hourly DO levels lower than 2 mg/l - of 86 %. The use of predictors extracted from a numerical hydrodynamic model allows us to overcome the intrinsic limitation of machine learning modelling approaches which rely on input data from relatively few, local field measurements, i.e. the inability to capture the spatial heterogeneity of DO distributions, unless several measuring points are available. The methodological approach is proposed for application to similar eutrophic environments.

* Corresponding author.
E-mail address: irene.simonetti@unifi.it (I. Simonetti).

https://doi.org/10.1016/j.scitotenv.2024.175424
Received 7 June 2024; Received in revised form 19 July 2024; Accepted 7 August 2024
Available online 12 August 2024

1. Introduction

Dissolved Oxygen (DO) is a crucial parameter related to water quality in rivers, lakes, and coastal basins. Hypoxia occurs when the DO level is too low for the proper functioning of the ecosystems, triggering the mortality of fish, loss in biodiversity, and impacting the surviving organisms through sublethal stresses (Vaquer-Sunyer and Duarte, 2008).

Oxygen concentrations in both the open ocean and coastal waters seem to have been progressively declining in the 20th century (Breitburg et al., 2018). Factors governing hypoxia are both of anthropic and natural origin (Caballero-Alfonso et al., 2015). One of the primary anthropogenic factors is nutrient input, which is a driver for coastal eutrophication, leading to an overproduction of organic matter, that increases the oxygen demand. There are several hypoxia drivers linked to climate, e.g., high temperature (which reduces oxygen solubility), the entity of rainfall and runoff (altering the freshwater input quantity and quality), and wind intensity (affecting the oxygen exchange with the atmosphere). Additionally, hydrodynamic factors also play a role (e.g., reduced horizontal advection and increased water residence time). Climatic and hydrodynamic factors contributing to hypoxia are deeply interrelated, as climatic factors may also induce hydrodynamic changes. The relative importance of these factors, as well as their interrelationship, is strongly site-specific, being fundamentally governed by the morphology and flushing characteristics of the basin under study.

The definition of hypoxia conditions is not unique, with alarm threshold ranging from 2 to 5 mg DO/l (Gobler and Baumann, 2016). Strong differences take place in the effect of low DO levels for different marine benthic organisms (Vaquer-Sunyer and Duarte, 2008): while the threshold of 2 mg DO/l is generally adopted to indicate fisheries collapse (Diaz and Rosenberg, 2008), loss of biodiversity may be experienced with significantly higher DO thresholds (Vaquer-Sunyer and Duarte, 2008).

Coastal lagoons are particularly susceptible to hypoxic phenomena, due to their reduced rate of water exchange with the sea, low thermal inertia, limited water depth, high biological productivity, and significant anthropogenic pressure (Newton et al., 2014). Examples of such anthropogenic pressure include pollution and nutrient supply from industry, intense fishing (Shumka et al., 2023) and agriculture activity in the watershed (Rodríguez-Gallego et al., 2017), which are superposed to possible alterations of the ecosystem caused by climate change (Boateng et al., 2020; Rodrigues et al., 2021). The mutual interaction between these elements affects the eutrophication processes, the water quality of coastal lagoons, and DO in a complex way, whose prediction and understating are challenging tasks for many modelling applications.

Coupled hydrodynamic and hydro-ecological physically based numerical models (deterministic models hereafter) for simulating the most relevant ecological processes involved in the DO dynamics for lagoons have been developed and applied in the last decades (e.g. Béjaoui et al., 2017; Hull et al., 2008; Seiler et al., 2020). Deterministic models rely on a chosen set of processes considered crucial for the studied dynamics. These models can only predict effects that stem from the explicitly included processes. Typically, deterministic models are computationally demanding, require large amounts of data that are often hard to obtain and involve lengthy site-specific calibration steps.

Data-driven methods and Machine Learning (ML) applications gained significant consideration in the latest years, for water quality studies for inland waters (e.g. Arrighi, 2023; Bui et al., 2020), as well as for modelling a wide variety of marine and coastal phenomena (as recently reviewed in Pourzangbar et al., 2023 and Rubbens et al., 2023). ML-based methods represent the information contained in the data, regardless of the underlying processes, and can therefore reproduce the effect of relationships and dependencies that are not explicitly included in a deterministic model. Approaches based on the Random Forest (RF) algorithm (Breiman, 2001) have shown to be effective, as proved by the different successful applications in the literature briefly recalled hereafter.

An RF regression approach to predict DO levels offshore and nearshore the coast of California was used by Valera et al., 2020. Time, temperature, salinity, water depth, and wind were used as predictors. Very good performance was found in predicting DO concentrations with RF models trained on data from one particular site (R^2 of 0.99), but the performance was lower when the model trained for one site was used in another nearshore site (R^2 between 0.42 and 0.70). Gogoi et al. (2024) applied an RF model to predict chlorophyll-*a* in a micro-tidal estuary, using as predictors a set of physical and bio-geochemical water parameters, and obtained an R^2 of 0.47 with measured data. Liang et al., 2023 compared the performance of different tree-based methods for predicting DO concentrations in Mirs Bay (Hong Kong), with R^2 between 0.7 and 0.79.

Specifically for coastal lagoons, Béjaoui et al. (2016) applied the RF algorithm to formulate a predictive model for chlorophyll-*a* based on measured physicochemical variables for Bizerte Lagoon (Tunisia), with satisfactory prediction capability ($R^2 = 0.51$). The RF modelling to assess the trophic status of Ghar El Melh Lagoon (Tunisia) was also tested by Béjaoui et al. (2018). The authors suggested that the phytoplankton biomass in the lagoon could be efficiently predicted adopting silicates and temperature as main descriptors. Hadid et al. (2021) used a combination of neural networks and RF methods to predict and forecast chlorophyll-*a* in the North Lagoon of Tunis, with satisfactory performance ($R^2 \sim 0.79$ between predictions and measurements) when using as only predictors the water depth and DO. For Venice Lagoon (Italy), Zennaro et al., 2023, applied a hybrid framework based on ML algorithms (RF and multilayer perceptron) and a deterministic model of water quality to predict chlorophyll-*a* in future climate change scenarios. The authors highlighted the enhanced extrapolation and generalization capabilities of the ML approaches, which detect phenomena not captured by the causal relationships in the deterministic model. Politikos et al., 2021, tested the capability of four machine learning algorithms to forecast hypoxia in Papas Lagoon (Greece), finding superior performance of the tree-based ML methods compared to logistic regression. Ph, chlorophyll-a, salinity, temperature, and solar radiation were found to be the most relevant set of predictors of DO levels. These previous works suggest the great potential of RF-based ML techniques in predicting, and possibly forecasting, DO. ML-based approaches, however, need to rely on observed values of the input parameters, hindering the possibility of representing the spatial heterogeneity of DO distributions in a coastal basin, unless a wide number of measuring stations is available in the basin.

In this work, we explore the possibility of using an RF algorithm to predict DO levels in a shallow-water, eutrophic coastal lagoon. A methodology that combines RF and numerical simulations to capture the spatial heterogeneity of DO levels without using deterministic models is presented. To the best of the author's knowledge, such an approach has not been previously proposed in the literature. The RF algorithm is trained with a set of predictors derived, alternatively, from measurement stations located in the lagoon or from a model of the hydrodynamics and heat exchange processes (HD model hereafter), which also provides water temperature and salinity. Using predictors derived from the HD model enables a high-resolution spatially distributed identification of hypoxic areas. The original contribution of this work is twofold: (i) it explores the possibility of obtaining predictions of hypoxia in coastal lagoons, forecasting the events with relevant advance notice and without using deterministic hydro-ecological models; (ii) it investigates whether predictors derived solely from the HD model can effectively replace physical and chemical water quality measurements typically obtained from a limited number of in-situ measurement stations.

2. Study area

The effectiveness of the proposed methodology is tested on the Orbetello lagoon, a coastal basin located in Central Italy (between

42°25′ and 42°29′N and 11°10′ and 11°17′E). The lagoon is 26 km^2 wide and has a mean water depth of 1.13 m. It is connected to the sea through three channels, two in the northwestern areas of the lagoon (the Ponente basin) and one in the southeastern areas (the Levante basin), as indicated in Fig. 1. Each channel is about 2 km long, 10–15 m wide and up to 1.8 m deep.

The confined morphology and limited astronomic tidal range, generally lower than 30 cm, reduce the water exchange with the sea and the mixing of the lagoon waters. The lagoon is heavily used for fishing activities and the natural water exchange is further reduced by the presence of grids and gates in each channel, used for fishing purposes (Fig. 1, right). A set of pumps, generally activated in the spring and summer months, is installed in each channel to promote the water exchange with the sea. The water residence time (WRT) of the lagoon has been estimated up to 200–230 days for the natural circulation, reduced to around 60 days when activating the pump systems (Zannella et al., 2024; Simonetti and Cappietti, 2022).

The lagoon is a remarkedly eutrophic environment (Soria et al., 2022), due to both its morphological features, the low water turnover, and the anthropic pressure to which it has been subjected over the years (Lenzi et al., 2003). The lagoon receives the treated discharge from two intensive aquaculture plants located inland, and until a few years ago, treated wastewater was also discharged into the basin (Lenzi et al., 2013). The sediments on the lagoon bottom have progressively enriched in nutrients. Recurring anoxic crises have been documented in the lagoon since the 1960s, with several massive fish die-offs over the last decades.

Physical-chemical water parameters monitoring stations (PCS), one located in the centre of the Ponente basin and two in the Levante basin (Fig. 1, left), collect hourly data on temperature, salinity, pH, Redox potential, and DO. Hourly values of meteorological parameters (wind speed and direction, solar radiation, air temperature, atmospheric pressure, relative humidity, precipitation, and clearness) are collected at the meteorological station located on the Orbetello isthmus (MS station in Fig. 1). The salinity in the lagoon has important seasonal variation cycles, with a progressive increase from the winter values of around 30 PSU (i.e. lower than that of the open sea) to the summer values of around 45 PSU (higher than the open sea ones), mainly due to a progressive increase of the evaporation. Water temperature ranges from approximately 5 to 35 °C. In the summer months, daily mean temperatures higher than 30 °C are frequently recorded. Daily mean values of DO generally range between 8 and 12 mg/l in the winter and 2 and 8 mg/l in the summer, with a typical eutrophic daily oscillation that often exceeds 6 mg/l (Fig. 2), transitioning from anoxic conditions in the early morning to states of oversaturation due to algal oxygen production during daylight hours.

3. Methods

The overall methodology adopted in this work is depicted in Fig. 3 and briefly summarized hereafter.

A Random Forest (RF) classification algorithm is used, aiming to predict the hourly classification of DO concentration into one of four distinct categories:

- Very low, DO $<$2 mg/l
- Low, 2 $\leq$ DO $<$4 mg/l
- Medium, 4 $\leq$ DO $<$8 mg/l
- High, DO $\geq$8 mg/l

The class Very low corresponds to the threshold generally identifying severe hypoxia, a proxy of fish collapse (Diaz and Rosenberg, 2008), while the Low class denotes the upper threshold for hypoxia (Gobler and Baumann, 2016).

We developed two sets of RF models. The first one (RF-MEAS hereafter) is trained with spatially uniform physical parameters over the lagoon and data from the three PCS located in the lagoon (Ponente, Levante2 and Levante stations, as in Fig. 1), which also provide hourly observations of DO concentration. The complete list of the available potential predictors is provided in Fig. 3 and further explained in *Section 3.2*. The possibility of using the RF-MEAS model to forecast hypoxic episodes was then explored by building a set of classification models trained with time-lagged predictors, i.e. correlating the class of DO at the instant *i* with the predictors at the time *i-N*, with *N* varying between 12 h and 10 days.

The second set of RF models (RF-HD hereafter) used the same

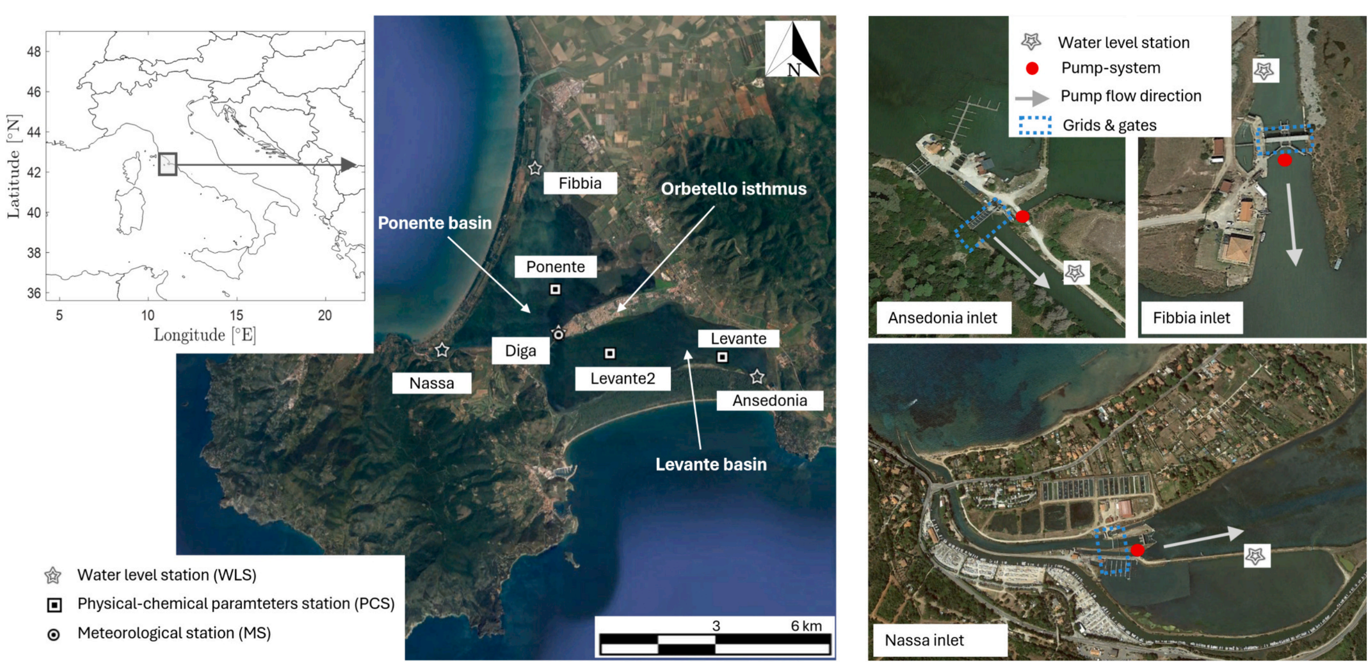

Fig. 1. Geographical location of the Orbetello lagoon and monitoring stations within it (left); close-up views of the lagoon inlets, with the location of the water pumping systems and of the grid and gates system to prevent fish escape.

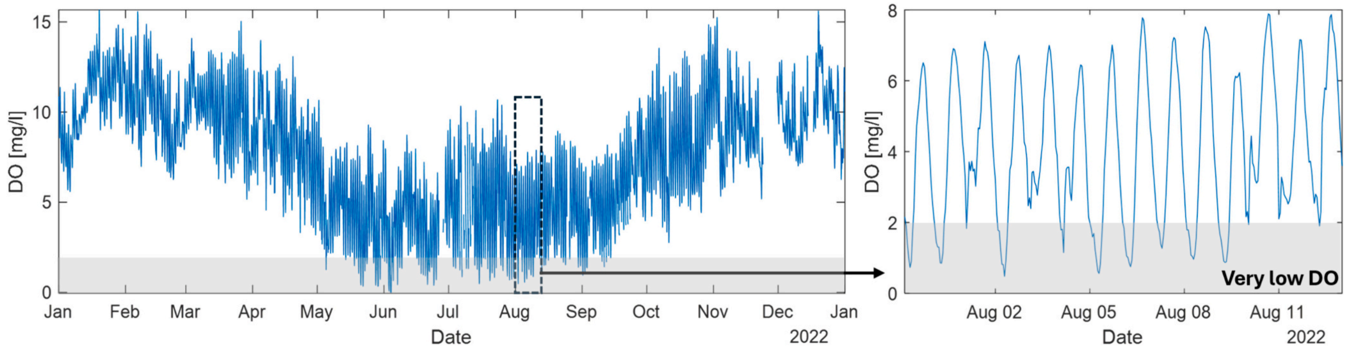

Fig. 2. Example of time series of hourly DO concentration recorded at the Ponente PCS measurement station for the year 2022. Highlighted in grey: DO levels <2 mg/l (i.e., the Very low class and threshold for hypoxic conditions).

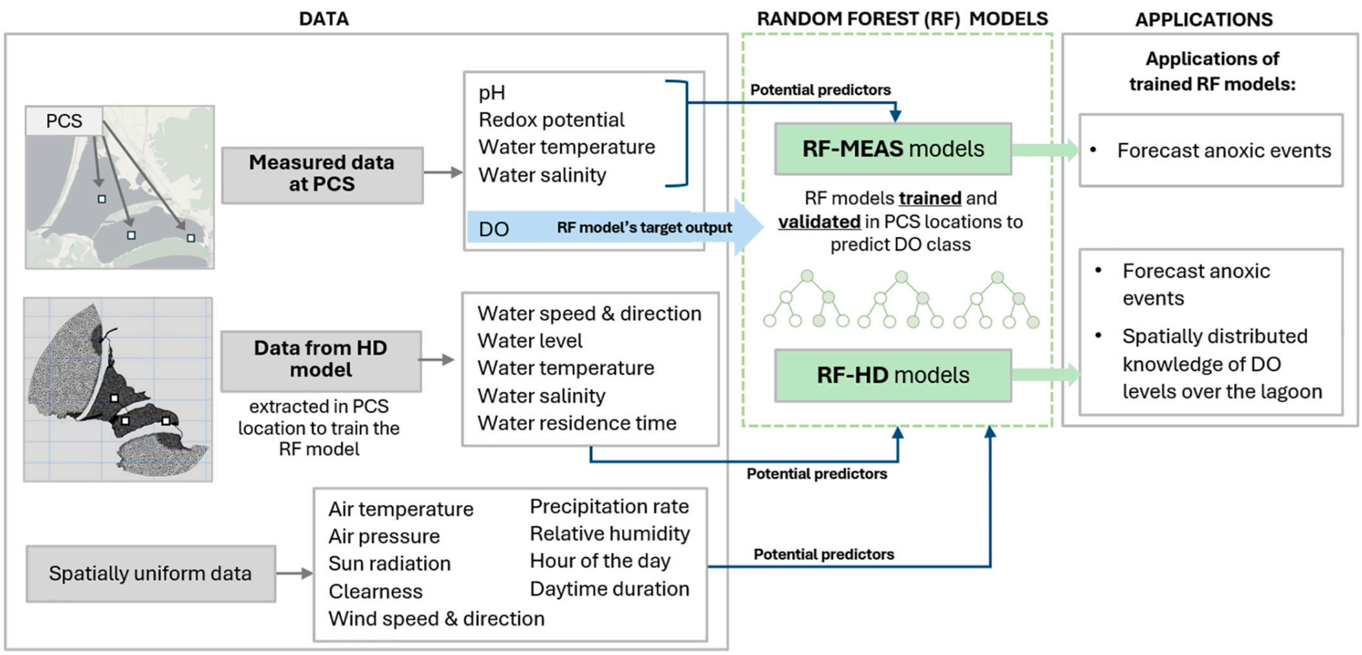

Fig. 3. Overview of the general methodology applied in this work; PCS: physical-chemical parameters measuring stations within the lagoon.

spatially uniform physical parameters as the RF-MEAS models and a larger set of predictors obtained from the hydrodynamic and heat exchange model of the lagoon (the HD model), as a replacement for predictors obtained via the in-situ measurements. RF-HD models were trained to predict DO at the same three PCS locations, i.e. where DO measurements are available and numerical data are extracted from the HD model. After having trained the RF-HD models, we made the strong assumption that a model trained based on data from the three PCS locations could later be applied to predict the DO class at any other location in the lagoon. This assumption relies on the availability of predictors derived from the HD model in each computational cell, which has a spatial resolution of around 80 m. Such an assumption is verified and discussed in *Section 4.5*. The possibility of forecasting hypoxic events was also explored with the RF-HD models.

This methodological approach, which integrates RF and HD models, enables the reconstruction of spatial heterogeneity in DO levels across the lagoon. The HD model is described in *Section 3.1*, while the predictors and datasets for training and validating the RF-MEAS and RF-HD models are presented in *Section 3.2*. Details on the RF algorithms and training procedures are given in *Section 3.3*.

3.1. Hydrodynamic model and heat exchange model of the lagoon

For the HD model, we used the Hydrodynamic Flexible Mesh (FM) module of the MIKE21-DHI software package. The model solves the fully non-linear and depth-averaged shallow water equations, with an eddy viscosity-based closure for turbulence, also simulating the heat exchange with the atmosphere and the transport–diffusion for water temperature and salinity. In-depth details on the development, calibration and validation of the model are given in Zannella et al. (2024) and Simonetti and Cappietti (2022). Only the salient features are described here, for the sake of completeness. The unstructured grid combines triangular and quadrangular elements with sizes varying between 2 m (in the inlets), 80 m (in the inner areas of the lagoon), and around 250 m outside the lagoon (Fig. 4). A constant Gauckler–Strickler coefficient of 30 $m^{1/3}/s$ is used for the bottom friction. The computational time step is dynamically adapted to maintain a Courant–Friedrichs–Lewy number lower than 0.8. Eddy viscosity is set to a value of 0.001 m^2/s. Hourly time series of water levels, temperature, and salinity are used as boundary conditions. Such data were extracted from the Mediterranean Sea Physics Analysis and Forecast database of Copernicus Monitoring Environment Marine Service (CMEMS) (Clementi et al., 2021), a coupled regional wave-hydrodynamic model covering the whole

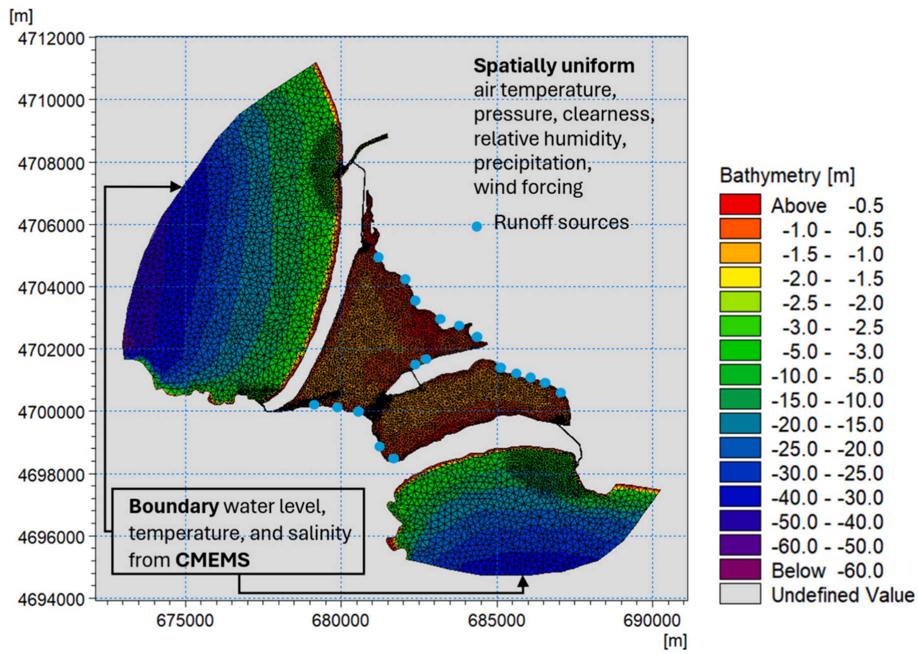

Fig. 4. Computational domain and grid of the hydrodynamic and heat exchange model used in this work, with the indication of the bathymetry of the area of interest, the boundary conditions, and the forcings used in the model.

Mediterranean Basin. Hourly observations recorded at the meteorological station at the lagoon center (Fig. 1) (i.e. wind, air temperature, relative humidity, precipitation, and clearness) are used to model heat exchange with the atmosphere. Such data are assumed spatially uniform over the whole domain. Runoff from the different sub-catchments is introduced as a set of point sources along the land boundary of the lagoon (see Fig. 4). The hourly values of runoff were obtained based on the application of the EPA Storm Water Management Model (SWMM) (Rossman and Huber, 2016).

The pumping stations in the inlets are simulated as an ensemble of mass sources and transversal structures across the inlets to limit the water outflow (gates), allowing the reproduction of a specific pump's characteristic curve. The model was validated by comparing hourly values of numerical results and field measurements for the years 2020 to 2022 (Zannella et al., 2024), obtaining a Root Mean Square Error (RMSE) of 0.025–0.04 m on the water levels (slightly varying for the different water level stations), an average RMSE of 1.2 °C on water temperature and 2.4 PSU on salinity (regarding the stations of Levante, Levante2, and Ponente, Fig. 1).

3.2. Datasets

The dataset used to train and validate the RF-MEAS models (*Dataset MEAS*) contained hourly observations relative to the years 2020, 2021, and 2022, of the following variables:

- Physical-chemical parameters collected at the three PCS stations in the Lagoon (Ponente, Levante and Levante2 station in Fig. 1), i.e.: hourly values of DO (used as the target output to be predicted by the RF model), pH, Redox potential, water temperature and salinity (used as predictors).
- Physical parameters spatially uniform over the lagoon, obtained from measurements at the meteorological station located at the centre of the lagoon (Diga station in Fig. 1), i.e.: hourly values of air temperature, atmospheric pressure, solar radiation, wind speed and direction, clearness, precipitation rate, relative humidity. Additionally, the hour of the day (expressed as in a 24-hour clock) and the daytime duration (i.e. the time elapsed between the beginning and the end of the sunshine period, in minutes, astronomically determined at the location of interest, disregarding cloud effects) were also considered as potential predictors, uniformly distributed over the lagoon.

As for the RF-HD models (*Dataset HD*), the dataset used for training and validation was composed of the following parameters:

- Hourly data of water level, velocity, temperature, salinity, and water residence time (WRT) derived from the HD model.
- The same spatially uniform parameters used in the *Dataset MEAS*.

Parameters such as time (hour of the day) and daytime duration were included as potential predictors to account for factors connected to the photosynthetic activity of the aquatic vegetation. This need is particularly intense, given the significant circadian variability of the DO in a eutrophic environment such as the Orbetello Lagoon, where the daily oscillations of DO in the summer months are high (Fig. 2). No other explicit parameter was included in the model to account for this phenomenon.

The most appropriate predictors to be used in the RF models were selected from the complete set of potential predictors in the *Dataset MEAS* and *Dataset HD* with a recursive feature elimination procedure (*Section 3.3.3*). For both datasets, the target output variable, i.e. the DO concentration, was provided by the hourly observations at the PCS stations. Around 60,000 observations are available in both datasets.

3.2.1. WRT as a time and space varying parameter

The predictive performance of the WRT to classify DO levels was assessed. The WRT is defined as the time it takes, in each point of the lagoon, for the concentration of a passive tracer initially homogeneously distributed with a concentration C0, to decrease to the value 1/e·C0 via advection/diffusion processes (Cucco and Umgiesser, 2006). Long WRT has been correlated to a higher risk of accumulation of nutrients (Ascione Kenov et al., 2012) and it is potentially predictive of low DO conditions (Coffin et al., 2018). WRT is naturally varying in space, i.e. WRT = f(*X,Y*), denoting with *X, Y* the 2D Cartesian Coordinates of the selected location in the lagoon.

In a specific location, the WRT changes over time, as it depends on the rate at which water is replaced, which is, in turn, influenced by the intensity of the hydrodynamic processes in the lagoon. In the Orbetello lagoon, the primary drivers of hydrodynamics are the astronomical and meteorological tides, wind conditions, and the operation of inlet pumps which are activated in the spring and summer seasons. All these factors greatly vary over time (as discussed recently in Zannella et al., 2024).

We proposed a time and space-varying WRT indicator obtained from simulations with the HD model as follows. For each instant t, with a discretization in time Δt, WRT(X,Y,t) was obtained from a simulation in which a tracer was released at the instant t-N (with N being a reference past period to be a priori chosen), which ran for a time N. In this work, $\Delta t = 1$ month and $N = 3$ months were chosen, as lower values of N would not allow for the decrease of the tracer concentration to the threshold value defining the WRT over vast areas of the basin. Values of WRT available with the time resolution Δt were later linearly interpolated to match the time resolution of the *Dataset HD* (i.e. 1 h).

3.3. Random forest classification algorithm and performance metrics

The Random Forest (RF) ML algorithm originally developed in Breiman, 2001, was used as a classification method to predict the hourly class of DO in a given location in the lagoon. The RF algorithm was chosen for its proven good performance for similar applications, due to specific features i.e. its non-parametric nature, the capability to handle correlated data affected by noise, and both numerical and categorical data. At a basic level, the RF method consists of building an ensemble of decision trees using a bagging method, i.e. creating different training subsets from the sample data, with replacement. Each tree makes a prediction (i.e., the class of DO concentration for the case at hand) and the final prediction is made based on the majority of predictions from the individual trees. The use of multiple decision trees allows for increasing the robustness to noise and outliers, reducing the instability of the single decision tree and limiting the problems of overfitting (Tyralis et al., 2019; Valera et al., 2020). RF algorithms may, on the other hand, decrease the interpretability of the predictions compared to single trees (Ziegler and König, 2014).

The RF models were developed by using the *Classification Learner* toolbox provided in Matlab®, adopting a staged approach, beginning with a preliminary database preparation, followed by hyperparameter tuning, a training stage, and recursive feature elimination (RFE) procedure to select the most appropriate predictors and a final testing stage.

3.3.1. Preliminary data preparation and SMOTE

The databases (MEAS and HD) have been preliminary treated to remove anomalous values most probably due to sensor errors. For training the ML algorithm, datasets were divided into a training dataset (70 % of the data) and a validation dataset (30 % of the data).

RF classification algorithms can be prone to issues when relevant differences in the number of observations in the classes take place (the so-called class imbalance, López et al., 2013). The minority class, having a lower number of data, is often the main focus of attention. This is indeed the case of the Very low class (DO <2 mg/l) in this study: observations of DO belonging to this class are around 4000 over a total of 60,000 observations available in the dataset.

In this work, in the database preparation, a synthetic minority oversampling procedure (SMOTE, Chawla et al., 2002), widely used in the literature to deal with such issues (Elreedy and Atiya, 2019), was applied to the training datasets. At a basic level, the SMOTE procedures consist of picking samples of the minority class and generating synthetic samples along the segment connecting the k nearest neighbours, randomly choosing neighbours from the nearest ones based on the specified oversampling rate required. The algorithm coded by Larsen (2024), based on the work of Chawla et al., 2002, was used. The minority class (i.e. the Very low class) was oversampled at 120 % of its original size, considering $k = 5$ nearest neighbours.

3.3.2. Performance metrics for the RF algorithms

The performance of the ML model was characterized in terms of overall accuracy (AC), which represents the percentage of observations that are correctly classified by the model (ratio of the correct predictions to all the predictions). The performance of ML algorithms was also evaluated by confusion matrixes, which compare the actual class of the observations with that predicted by the model.

For each class, the True Positive Rate (TPR), or recall, is the ratio of the number of DO occurrences correctly classified as belonging to a given class (true positive, TP) to the total number of observations belonging to that class (TP + FN, with FN being false negative). The False Negative Rate (FNR) is the ratio of the DO incorrectly classified as not belonging to a given class (false negative, FN) to the total number of observations in the class (TP + FN). The Positive Predicted Value (PPV), or precision, is the ratio of true positive TP to the total number of elements classified by the model as belonging to that class (TP + FP, with FP denoting false positive). The F1-score for class i is defined as the harmonic mean of TRP and PPV, as in Eq. (1).

$$F1_i = \frac{2}{\frac{1}{TPR_i} + \frac{1}{PPV_i}} \tag{1}$$

In the following, the confusion matrices report the TPR for each class along the diagonal elements and the FNR on non-diagonal elements.

3.3.3. Recursive feature elimination

Starting from the complete set of potential predictors in the *Dataset MEAS* and *Dataset HD*, a recursive feature elimination (RFE) procedure was employed to select the most relevant ones, i.e. the sub-set allowing to maximize the performance of the RF models. The RF models were initially trained on the complete set of predictors, calculating the related performance metrics. Next, using SHAP (Shapley Additive exPlanations) values (*Section 3.3.4*) to rank feature importance, the predictors were removed one at a time, starting with the least significant. After removing the predictor, the RF algorithm was retrained. If the performance of the newly trained RF model was higher or equal without the predictor, it was removed from the dataset, otherwise, it was retained. In this procedure, the indexes used to assess the performance of the model were the overall model accuracy AC and the TPR of the class Very low, i.e. TRP_{VL} (since this class is generally the greater focus of the attention). The procedure was repeated for all the potential predictors.

3.3.4. Feature importance and SHAP values

ML algorithms frequently face criticism due to their lack of interpretability. Understanding the rationale behind a machine learning model's prediction holds significant importance, as it fosters deeper comprehension of the process being modelled and trustworthiness in the ML model itself. SHAP-based methods (Lundberg and Lee, 2017; Lundberg et al., 2019) have been recently proposed for interpreting the output of ML models. Inspired by cooperative game theory, at a basic level, the SHAP approach quantifies the impact of each predictor by comparing the output of an ML model with and without that predictor. In recent years, SHAP has seen an upsurge in adoption across various ML applications (e.g. Politikos et al., 2021; Wang et al., 2021). For each predictor, the SHAP value Φ_i is computed as the difference in the model's prediction f_x when excluding or including the predictor i, averaged across all possible permutations of the predictor's subset (since the effect of excluding a predictor depends on the set of the other predictors), as in Eq. (2)

$$\varnothing_i = \sum_{S \in F \setminus \{i\}} \frac{|S|!(F - |S| - 1)!}{F!} [f_x(S \cup \{i\}) - f_x(S)] \tag{2}$$

where F is the complete number of model predictors, S is a predictor subsect from all predictors excluding i, $\frac{|S|!(F-|S|-1)!}{F!}$ is a weight factor accounting for the number of permutations in the subset S, $f_x(S \cup \{i\})$ is the expected output of the model when predictor i is included, $f_x(S)$ is the model output excluding the predictor i. In this work, SHAP values have been calculated based on the kernelSHAP algorithm (Lundberg et al., 2020) as implemented in Matlab® version 2024a.

4. Results

4.1. Classification algorithms using field measurements (RF-MEAS)

Using the RFE procedure introduced in *Section 3.3.3*, the subset of $p = 8$ predictors in Table 1 was adopted for training the RF-MEAS model for classifying DO levels by using data from measurement stations and spatially uniform data only, assuming no time lag between the predictors and the output ($N_{lag} = 0$). The final predictors were: water temperature, salinity, pH and Redox potential, air pressure, sun radiation, hour of the day, and daytime duration. The model was trained with the following hyperparameter options:

(i) number of weak learners (trees) to be bootstrap-aggregated, $NoL = 90$; NoL was selected as the number that approximately stabilized the performance of the RF algorithm.
(ii) number of predictors randomly selected for each decision split, $m=\sqrt{p}$ (being p the total number of predictors, as suggested e.g. in Hastie et al., 2009).

The trained RF-MEAS model has an overall accuracy of AC = 91 %, with the confusion matrix reported in Fig. 5a. The model can correctly identify 88 % of the occurrence of DO values belonging to the class Very low (hourly average value of DO<2 mg/l), i.e. $TPR_{VL} = 88$ %. 9 % of the occurrence of DO values in the Very low class are, instead, misclassified as belonging to the Low class, and 3 % to the Medium class. The recall of the model in identifying DO in the classes Medium and High is >90 %, while performance is minimum for the class Low (TPR = 69 %). Targeting the class Very low, the F1-score of the model, defined as in Eq. (1), is 89 %.

As a side note, the RF-MEAS model trained excluding the hour of the day from the predictors would result in a decrease in the classification performance of the model, particularly relevant for the DO class Very low (with TRR_{VL} decreasing to 80.8 %).

4.2. Classification algorithm using data derived from the HD model (RF-HD)

The predictors selected for the RF models trained with data from the HD numerical model and spatially uniform measurements (RF-HD models) by using the RFE procedure are reported in Table 1. The selected predictors derived from the HD model are: water temperature and salinity, water levels, and WRT (obtained as in *Section 3.2.1*). In addition, the same set of spatially uniform parameters adopted in the RF-MEAS model is also selected for the RF-HD model, e.g.: air pressure, hour of the day, and daytime duration. Using this subset of predictors, the RF-HD model, trained with the same hyperparameter options described above (i.e. $NoL = 90$ and $m=\sqrt{p}$), shows the confusion matrix of Fig. 5b, with an overall accuracy AC = 90.7 % and true positive rate and F1-score for the class Very low of $TPR_{VL} = 86$ % and F1 = 86 %, respectively. The classification performance of the RF-HD model is, therefore, comparable with that of the RF-MEAS model, allowing an estimation of the DO in each location of the lagoon, not being constrained by input parameters coming from the relatively few in-situ measuring stations installed at specific lagoon locations.

Including the WRT among the predictors increased TPR_{VL} from 80 % to 86 %, allowing the RF-HD model to achieve performance comparable with that of the RF-MEAS models.

Table 1
Final set of predictors of the RF-MEAS and RF-HD models selected after the Recursive Feature Elimination procedure.

Predictors of the RF-MEAS model	[unit]	Predictors of the RF-HD model[a]	[unit]
Water temperature	[°C]	Water temperature HD	[°C]
Water salinity	[PSU]	Water salinity HD	[PSU]
Water pH	[H+]	Water level HD	[m]
Water REDOX	[mV]	WRT HD	[days]
Air pressure	[atm]	Air pressure	[atm]
Sun radiation	[W/m^2]	Sun radiation	[W/m^2]
Hour of the day	[0–23]	Hour of the day	[0–23]
Daytime duration	[minutes]	Daytime duration	[minutes]

[a] Predictors derived from the numerical model of the hydrodynamics and heat exchange processes in the lagoon are denoted by the suffix HD.

4.3. RF models to forecast hypoxic events

We explored the possibility of using the RF-based approach to forecast DO in the lagoon with advance notice (N_{lag}) of 12 h to 240 h by training a set of models using time-lagged predictors, i.e. correlating the class of DO at time i with predictors at time i-N_{lag}. The same predictors selected with the RFE elimination procedure to train the models with $N_{lag} = 0$ h were maintained, as well as the RF algorithm hyperparameters. The performance of the RF-MEAS and RF-HD models, with different time lags, are shown in Tables 2 and 3, respectively. For the set of RF-MEAS models, the overall accuracy in DO classification AC decreases only moderately when increasing the time lag between predictors and predicted variables, with AC = 91 % for $N_{lag} = 0$ h and AC = 89 % for $N_{lag} = 240$ h. The F1-score on class Very low also slightly progressively decreases, with $F1_{VL} = 89$ % for $N_{lag} = 0$ h and $F1_{VL} = 86$ % for $N_{lag} = 240$ h. The recall and F1-score relative to the Low class (for which, as commented in the previous sections, performance is at a minimum also for the case of no time lag) decrease more markedly, with TPR_L varying from 69 % to 61 % and $F1_L$ from 73 % to 67 % for N_{lag} increasing from 0 to 240 h. Overall, the RF-MEAS models show satisfactory classification capability in forecasting DO levels up to 10 days in advance. The set of RF-HD models trained with time-lagged variables demonstrates enhanced stability of predictive performance with increasing forecast horizons, exhibiting no notable variation in accuracy for N_{lag} up to 240 h (Table 3).

4.4. Relative importance of predictors

Once the RF model has been trained, the relative importance of predictors in classifying and forecasting hypoxia was assessed based on SHAP values. To visualize the overall contribution of each predictor to the ML output, we considered the mean of the absolute SHAP values over all instances in the dataset (Fig. 6), indicating the relative importance of each predictor (the highest the mean of absolute SHAP values, the highest the relative importance of the predictor).

For the case of $N_{lag} = 0$, the most relevant predictors overall are, for the RF-MEAS model (Fig. 6a): pH, water temperature, hour of the day water, daytime duration, followed by water salinity and Redox potential. As far as the model conceived to forecast DO levels 240 h in advance is concerned (RF-MEAS with $N_{lag} = 240$ h, Fig. 6b), the ranking of the predictors is slightly modified, with the most relevant predictors overall being, in order of importance: daytime duration, hour of the day, pH, water temperature and salinity. Different predictors may have a different ranking of importance for different DO classes (e.g., pH, water temperature, and salinity equally contribute to the predictions for the class Medium, while water temperature and salinity are more relevant than pH for the class High).

As for the RF-HD models, the ranking of the five most relevant predictors is: water temperature, hour of the day, WRT, daytime duration and salinity when no time lag is considered between predictors and the output ($N_{lag} = 0$ h, Fig. 6c), changing to: daytime duration, salinity, hour of the day, WRT, and water temperature for the model to forecast DO

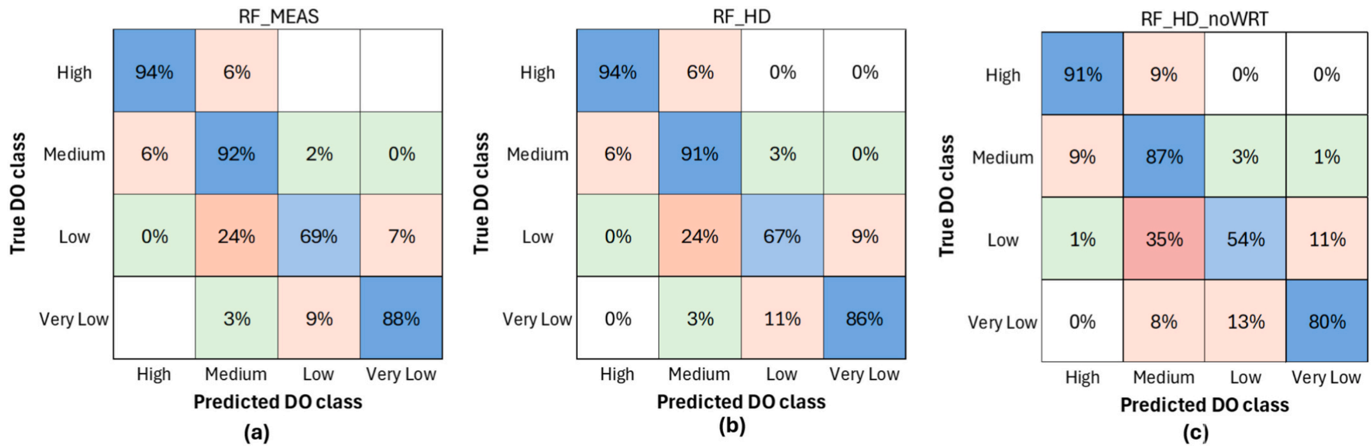

Fig. 5. Confusion matrix for the trained RF models with contemporary predictors and output ($N_{lag} = 0$): RF-MEAS model (a), RF-HD model (b), and RF-HD model without the inclusion of water residence time WRT among the predictors (c). Confusion matrixes have the True Positive Rate (TPR) on diagonal elements and False Negative Rate (FNR) on non-diagonal elements.

Table 2
Overall classification accuracy AC (%), true positive rate (TPR), positively predicted value (PPV) and F1-score for the performance of the RF-MEAS models to identify the classes Very low (subscript VL) and Low (subscript L) for time lags between predictors and output $N_{lag} = 0$ to $N_{lag} = 240$ h.

	RF-MEAS						
Time lag N_{lag}	AC	TPR_{VL}	PPV_{VL}	$F1_{VL}$	TPR_L	PPV_L	$F1_L$
0 h	91	88	91	89	69	78	73
12 h	89	85	88	86	62	75	68
24 h	89	85	87	86	62	74	67
48 h	89	85	88	87	62	74	67
96 h	89	85	87	86	60	73	66
240 h	89	84	87	86	61	74	67

Table 3
Overall classification accuracy AC (%), true positive rate (TPR), positively predicted value (PPV) and F1-score for the performance of the RF-HD models to identify the classes Very low (subscript VL) and Low (subscript L) for time lags between predictors and output $N_{lag} = 0$ to $N_{lag} = 240$ h.

	RF-HD						
Time lag N_{lag}	AC	TPR_{VL}	PPV_{VL}	$F1_{VL}$	TPR_L	PPV_L	$F1_L$
0 h	91	86	87	86	67	74	70
12 h	91	87	87	87	68	76	71
24 h	91	86	88	87	68	75	71
48 h	90	86	88	87	67	74	70
96 h	90	85	88	86	68	74	70
240 h	90	85	88	86	67	74	70

class 240 h in advance ($N_{lag} = 240$ h, Fig. 6d).

For both the RF-MEAS and the RF-HD models, the relevance of water temperature on the model output decreases when increasing N_{lag} (from the second to the fourth place for the RF-MEAS model and from the first to the fourth place for the RF-HD model), while daytime duration attains a greater relevance. For all considered models and time-lags, air pressure and sun radiation are the least relevant predictors.

The mean of absolute SHAP values only denotes the strength of the influence of a predictor on the output of the model but does not provide any indication of the qualitative direction of such influence, i.e. it does not show either a given predictor increases or decreases the likelihood of a prediction belonging to a given class. To address this aspect as well, SHAP summary plots for individual classes are also shown. For the Very low class, such plots are provided in Fig. 7. In these plots, each dot is the SHAP value of a given predictor at a given data point, with overlapping dots spreading along the y-axis direction. The colour scale indicates the value of the predictor for the data point, allowing for the identification of the most relevant predictors, as well as the nature of their influence on the model's outputs (positive or negative). When focusing on a specific class, positive SHAP values denote an increased probability of having a predicted value of DO falling into that class, while values close to 0 suggest a negligible impact of the predictor on the results.

For the RF-MEAS models, despite the value of the time lag N_{lag} (Fig. 7a, b), low values of pH are associated with an increased probability of having a prediction of DO belonging to the class Very low, while high pH values decrease the probability of a DO prediction in the same class. High values of water temperature, the second most important predictor for the RF-MEAS model and the first most important predictor for the RF-HD model with no time lag (Fig. 7c), show a clear increase in the risk of having very low DO predictions. As observed above for mean absolute SHAPs, the relevance of temperature on the predictions of DO levels as belonging to the class Very low decreases remarkably when considering longer forecast horizons (Fig. 7c, d). A long red tail on the right-hand side of the summary plot is, however, still well identifiable, denoting a persisting correlation between high temperature and hypoxia risk.

Greater values of daytime duration, which take place in the summer months, are associated with an increased probability of having a prediction by the RF models in the class Very low. This predictor is particularly relevant for $N_{lag} = 240$ h (i.e. for the 10-day forecast of DO levels), obtaining the first position for both the RF-MEAS and the RF-HD models. Low values of the hour of the day (which alternates between the third and the second position for importance in all models shown in Fig. 7), are associated with an increased probability of having DO predictions in the class Very low, according to the evidence that hypoxia takes place when the oxygen production of the chlorophyll photosynthesis is not present. Higher salinity values increase the probability of predicting a Very low DO, for both the RF-HD and RF-MEAS models and time lags. High values of the WRT, which is only used as a predictor in the RF-HD models, are associated with the highest SHAP values for the Very low class, with a long red tail of the distribution on the right-hand side of the graph. It is worth noting, however, that compared to other predictors (i.e. pH, temperature, and hour of the day), the predictive power of WRT appears to be more limited, since the majority of SHAP values are spreading around zero, despite the long tail of the distribution (Fig. 7c–d). This indicates that the feature in question is generally not very influential, but in some specific situations, it can have a significant impact on the model's prediction.

At the opposite end of the DO range, SHAP summary plots for the class High (DO ≥8 mg/l) are shown in Fig. 8. It is firstly worth noting

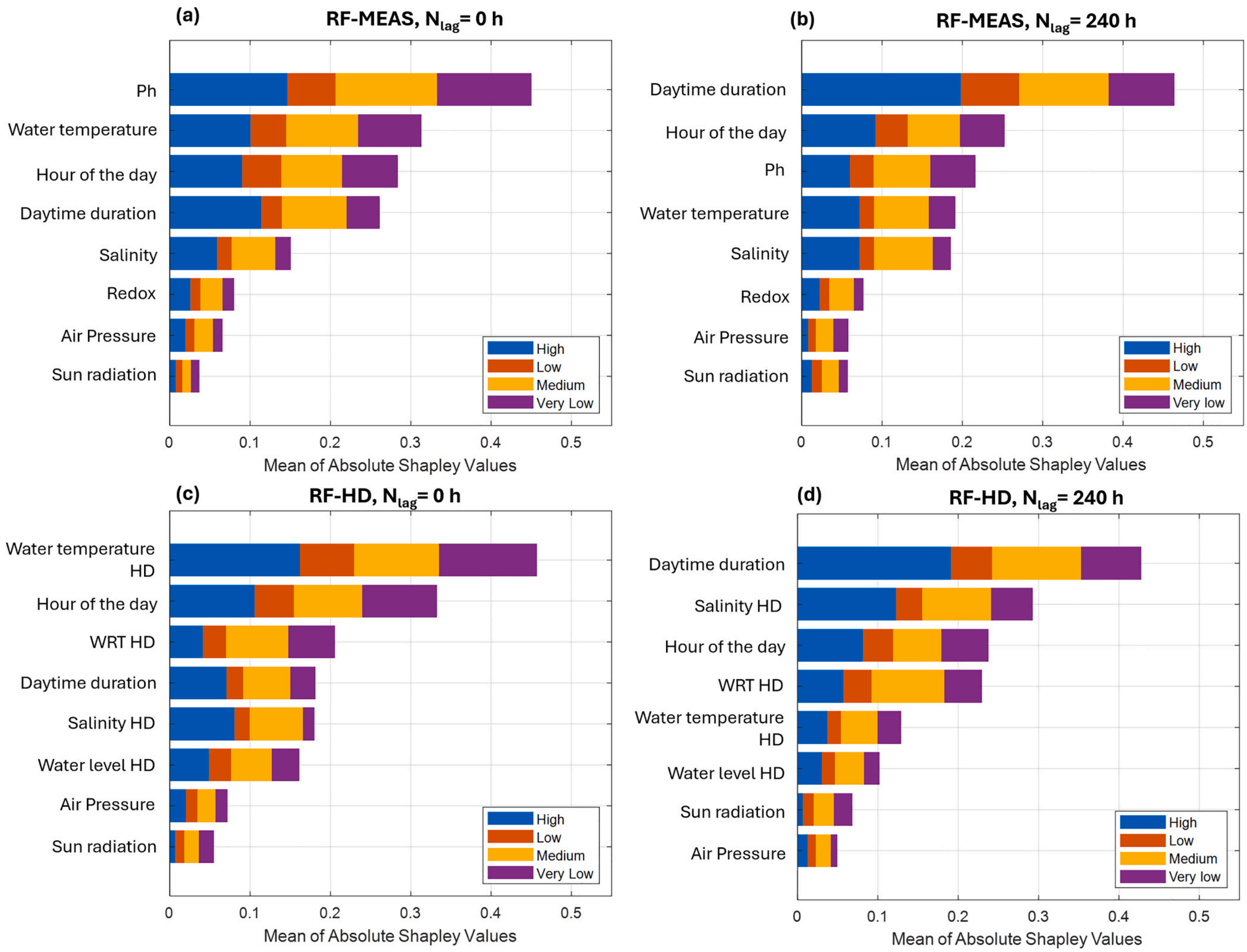

Fig. 6. Barplots of the mean of the absolute SHAP values of each predictor for the four DO classes, for the model formulated based on measured data RF-MEAS (a), (b) and data from the hydrodynamic model RF-HD (c), (d), with a time-lag between the observation and the prediction $N_{lag} = 0$ h and 240 h, respectively.

that in this case, for the most relevant predictors, the x-axis location corresponding to the maximum density of observations (i.e., where values are most littered along the y-direction) occurs corresponding to SHAP values that are farthest from zero relative to the Very low class. This denotes a higher impact of the predictors on the model output, consistently with the better predictive performance shown in Fig. 5 for this class. SHAP values for class High are highly consistent with those for class Very low. Lower values of daytime duration remarkably increase the odds of having a DO prediction in the class High, and this predictor is one of the most influential on the output of the RF model for all addressed cases, except for RF-HD with $N_{lag} = 0$, in which it is preceded in importance by water temperature, hour of the day and salinity. High pH values (Fig. 8a, b) increase the probability of having a High DO prediction with the RF-MEAS models, even if it is worth highlighting that the relevance of this predictor falls from the first to the fifth position when considering a forecasting horizon of 240 h. Low water temperature values are strongly correlated to a higher chance of predicting DO as belonging to the class High, with greater importance of the predictor for $N_{lag} = 0$.

SHAP summary plots for the other classes are not shown for the sake of brevity.

4.5. Example application of the RF-HD model to reconstruct the spatial distribution of DO during documented critical events

The RF models have been trained and verified concerning measurements available in the three physical-chemical parameters stations (PCS) located as in Fig. 1. The RF-HD model, however, allows obtaining a spatially distributed prediction of DO levels, since the predictors (which are either uniform over the lagoon or obtained from the HD model) are known at any point, with the same resolution in space of the HD model. To verify the extent to which the RF-HD model can be applied to represent the spatial heterogeneity of DO distributions over the lagoon, it was used to reconstruct DO levels for some critical events documented for the summer of 2022. For these events, maps of DO were available through an ad-hoc monitoring campaign commissioned by the Tuscany Region Authority (Leporatti Persiano, 2022). Such maps were extrapolated from field measurements conducted in a limited number of points, over some hours, and can be considered qualitatively representative of locations in which hypoxic conditions were particularly severe during the selected events. For the same periods, predictors from the HD model were extracted on a regular grid with a 250 m spacing over the lagoon and used to obtain an estimation of DO levels through the RF-HD model with $N_{lag} = 0$. The resulting maps are compared in Fig. 9. The RF-HD model was able to identify the occurrence of hypoxic areas for the considered events. In the first one (Fig. 9a), a large area with DO <2 mg/l was identified by measurements in the south-western side of the

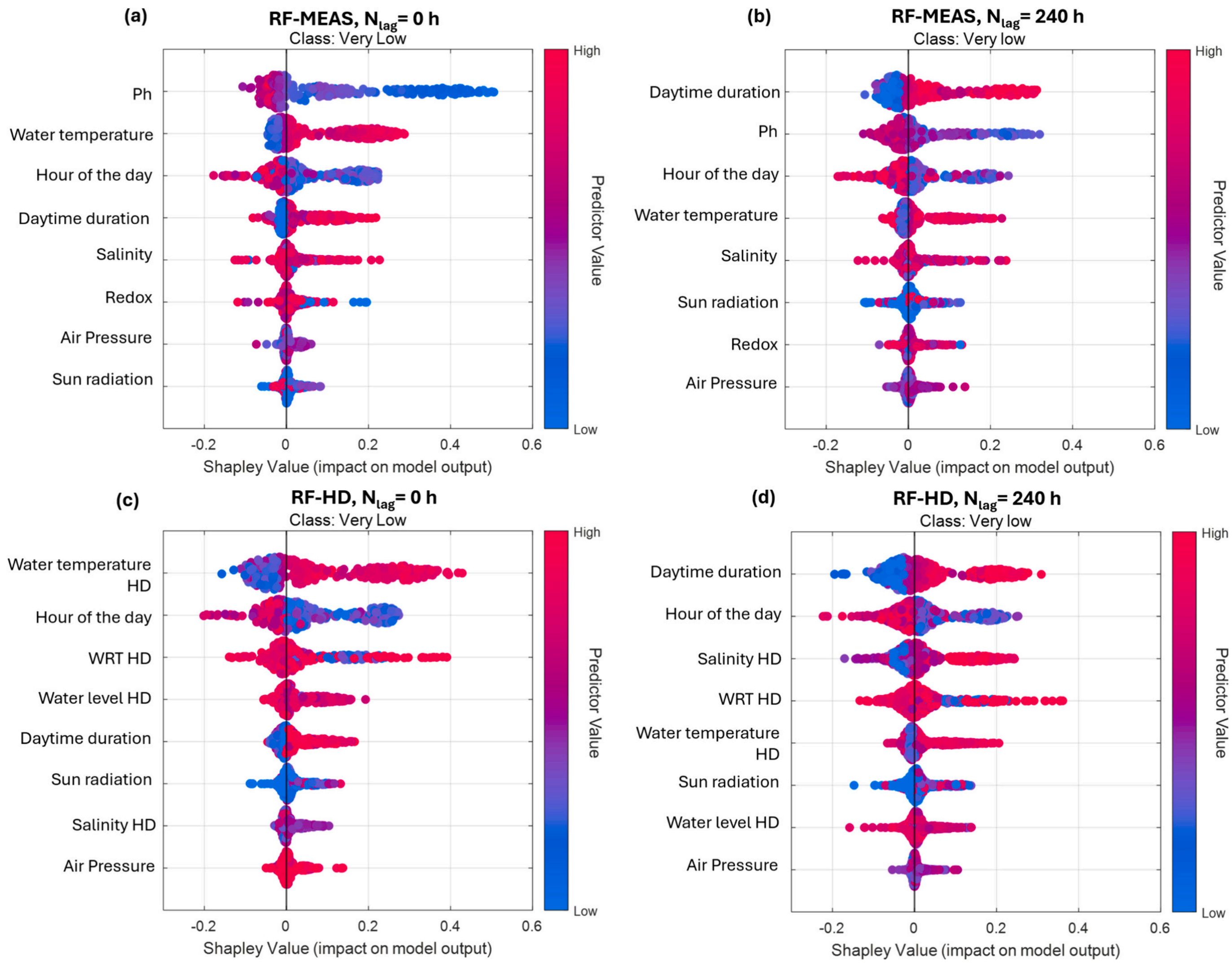

Fig. 7. SHAP summary plot for DO class Very low, for the model formulated based on measured data RF-MEAS (a), (b) and data from the hydrodynamic model RF-HD (c), (d), with a time-lag between the observation and the prediction $N_{lag} = 0$ h and 240 h, respectively.

Levante basin, with a low DO area in the Ponente basin, close to Orbetello isthmus. The model was able to identify the Levante basin as the one with the highest criticality and highlighted areas with Low DO levels in the Ponente basin, albeit with some spatial misalignments in the localization of the affected areas. Nonetheless, the model's performance is satisfactory, also considering that maps extrapolated from field measurements grant only qualitative spatial representativeness. Also for the second event (Fig. 9b), the model can locate, with satisfactory accuracy, two DO spots in the class Very Low located in the south-western end of the Levante basin and in the Ponente basin, adjacent to the central area of Orbetello isthmus. Some inaccuracies must be highlighted in the identification of the Low DO areas shown by field measurements, which are misclassified by the model as belonging to the Medium DO class. Although these data are not enough to support a comprehensive model validation, they indicate that the spatial distributions of DO generated by the model are plausible and align with observed measurements.

5. Discussion

5.1. Most relevant parameters in the RF models and consistency with previous studies and knowledge

Orbetello Lagoon is a strongly eutrophic environment. The well-known oxygen production and consumption processes determine the diel trend of DO concentration, with peaks during the day hours and variations driven by temperature and sunlight cycles, as well as by the balance of photosynthesis and respiration processes (D'Avanzo et al., 1996). On the contrary, during the night and early morning hours when sunlight is not available for photosynthesis, DO concentration tends to decrease. The interaction of all the aforementioned factors deeply affects DO fluctuations. In the RF models proposed in this work, biological activity is not explicitly included among predictors, however, a set of additional parameters, correlated to the strength and to the circadian oscillation of DO biological production were included in the model to contribute to account for these effects (e.g., hour of the day, daytime duration, solar radiation). The limitations arising from such an approach are further discussed in *Section 5.2*. The two parameters daytime duration and solar radiation, therefore, indirectly account for biological production in controlling DO and the organic patterns influencing diel hypoxia. Solar radiation, measured at the PCS at the lagoon's center, also accounts for the effective cloud cover in the area of interest. Cloud cover reduces photosynthetic activity, resulting in lower values of the maximum DO levels in the afternoon hours (Tyler et al., 2009). In these conditions, water may be not sufficiently oversaturated to accommodate the needs of DO for respiration in the following night and early morning hours. The total insolation of the previous day was found to be

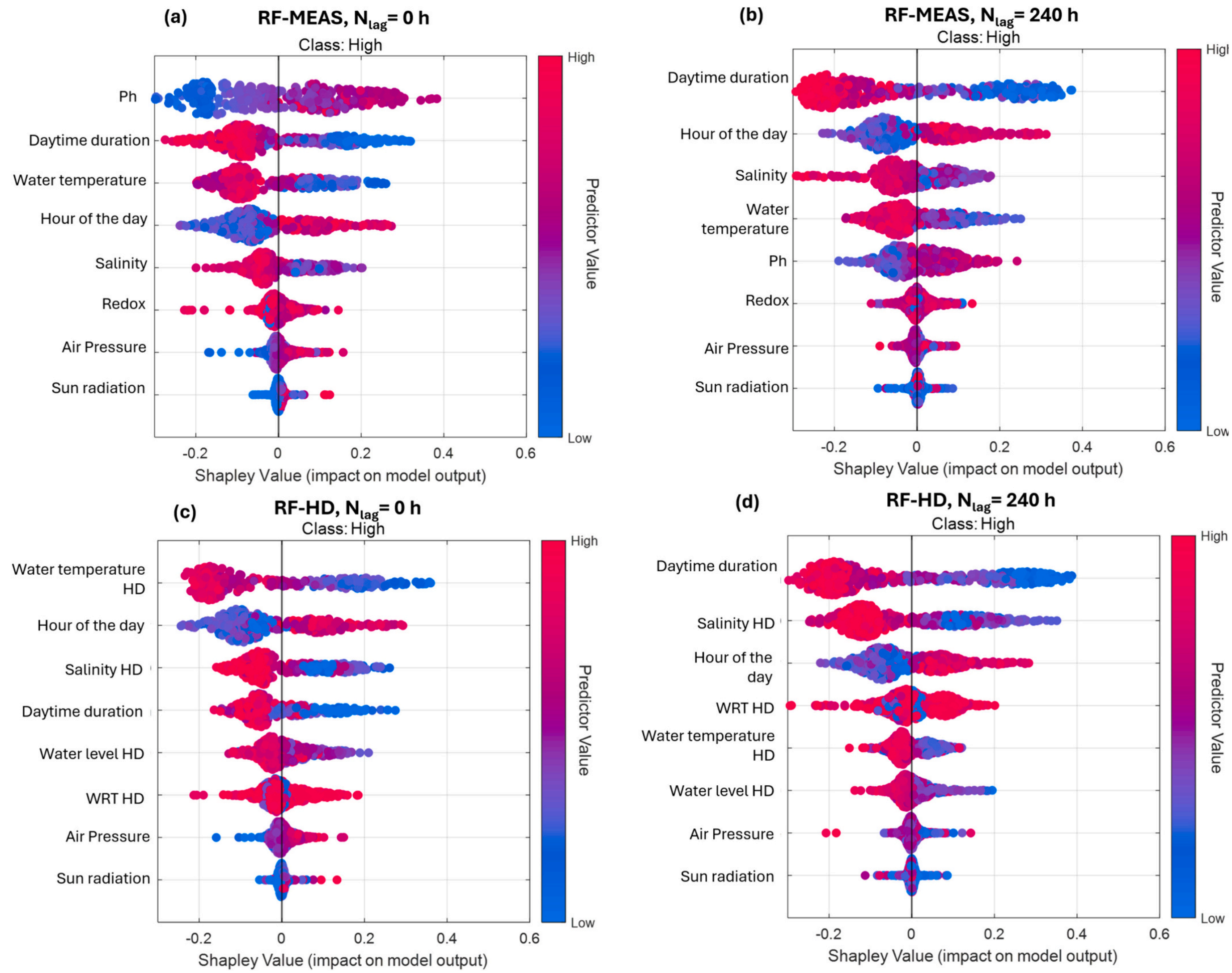

Fig. 8. SHAP summary plot for DO class High, for the model formulated based on measured data RF-MEAS (a), (b) and data from the hydrodynamic model RF-HD (c), (d), with a time-lag between the observation and the prediction $N_{lag} = 0$ h and 240 h, respectively.

particularly well correlated to the minimum DO level of the following day (Tyler et al., 2009). In the present work, the SHAP analysis revealed a growing relevance of both the daytime duration and the sun radiation when the time-lag increases from $N_{lag} = 0$ to $N_{lag} = 240$ h, for both the RF-MEAS and the RF-HD models (Fig. 7). The correlation of higher daytime durations with increased chances of having a Very low DO level is particularly evident. SHAP values offer a less straightforward interpretation of the role of solar radiation in the RF model predictions, reflecting the complex physical mechanisms through which it influences DO levels. On one hand, higher solar radiation values are characteristic of the summer period, serving as a proxy for hypoxia. On the other hand, as noted in the literature, cloudy days during the summer can limit diurnal photosynthetic activity, thereby exacerbating the risk of hypoxia in the night hours.

The relevance of pH as a predictor of hypoxic conditions, as well as the association of low pH values and hypoxia highlighted in this work (Figs. 7 and 8), is well supported in the literature for both ocean ecosystems in general (Gobler and Baumann, 2016; Melzner et al., 2013) and coastal lagoons (Politikos et al., 2021). Indeed, pH follows the same trend as DO: photosynthetic activity consumes CO_2, therefore increasing pH. In the absence of photosynthesis, CO_2 is emitted by respiration, with a corresponding decrease in pH. This relation is particularly evident in shallow-water coastal zones with high respiration rates, as the one at hand (Duarte et al., 2013). In addition, pH is linked to anaerobic conditions and sulphate reduction in the sediments (Cioffi et al., 1995) with the production of H_2S.

The SHAP analysis highlights an association between warmer temperatures and an increased risk of hypoxia, which aligns with well-established scientific findings. Higher temperature decreases the oxygen solubility in water (Garcia and Gordon, 1992). Temperature also increases biological activities, such as plant respiration and photosynthesis and microbiological degradation processes. Indeed, temperature is often assumed as one of the main controlling factors for the assessment of hypoxic conditions in marine environments (Roman et al., 2019). SHAP values show a correlation between higher salinity and a greater likelihood of having a DO prediction in the Very low class. This is also consistent with established knowledge, as an increase in salinity results in a reduction of DO, due to a decrease of the oxygen solubility in water at a given temperature and atmospheric pressure.

In the present study, wind was excluded from the set of predictors during the RFE stage, since its inclusion among predictors worsened the overall performance of the model. The wind action, however, is well recognized as one of the main factors driving hydrodynamics for coastal lagoons. For the Orbetello lagoon, this effect was studied by Zannella et al. (2024), who found a substantial contribution of wind-induced water circulation in lowering the WRT of the lagoon (which is reduced

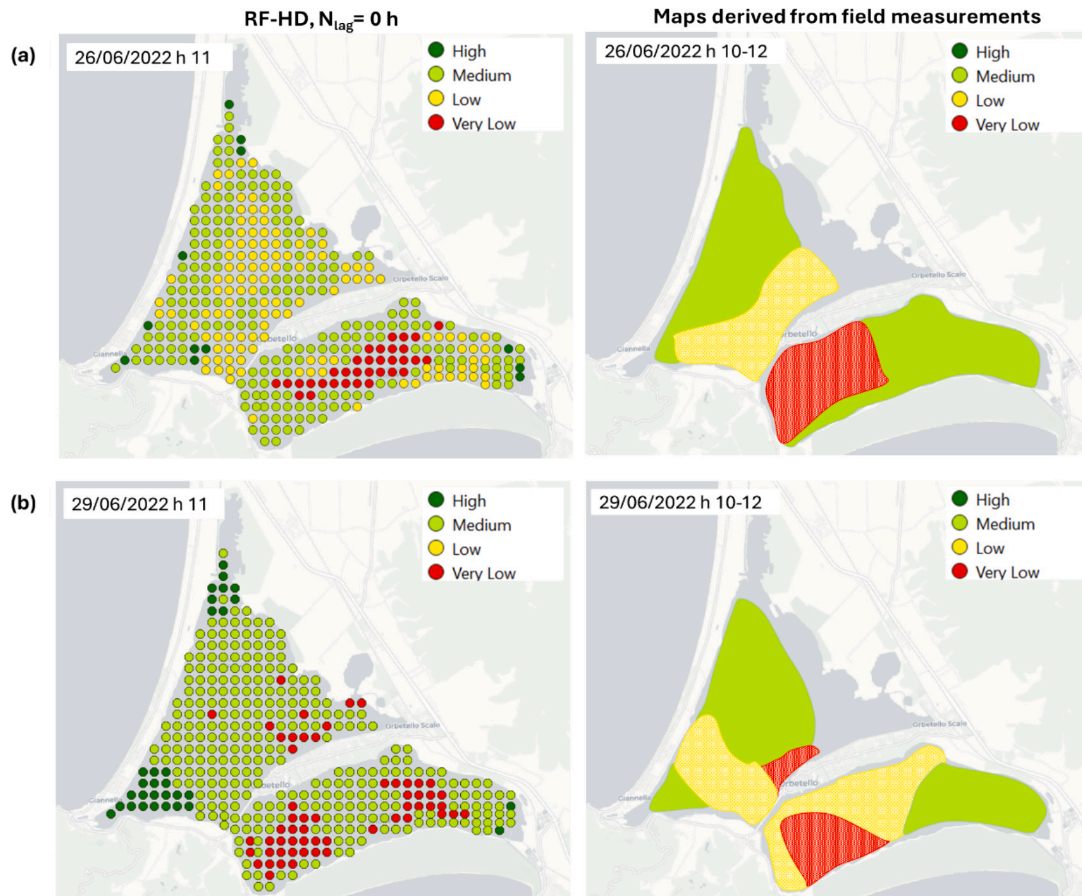

Fig. 9. DO levels as classified by the RF-HD model with $N_{lag} = 0$ (left) and as observed through field measurements in the lagoon (right) during two critical events with dates 26/06 (a) and 29/06 (b) 2022.

by >40 % due to the wind action compared to a no wind scenario). The limited relevance of the wind as a predictor for the RF models can be explained by considering its twofold effect on the lagoon processes: (i) wind contributes to resuspending bottom sediments, which frequently harbor organic matter, object of subsequent oxidative processes, leading to DO consumption (Arfi et al., 1993; Mauro Lenzi et al., 2016). This process is particularly relevant in shallow water environments, such as the Orbetello lagoon; (ii) wind acting at the liquid surface induces turbulence in the water column, facilitating gas exchange at the air-water interface (Ro et al., 2007). For sub-saturated water conditions, intensified gas exchange tends to increase DO concentrations. On the contrary, areas undergoing oxygen oversaturation due to strong photosynthetic activity are susceptible to experiencing an opposite oxygen decrease due to wind-induced gas exchange phenomena. These two wind-induced processes act on DO in opposite directions, potentially lowering the predictive capabilities of this parameter in classifying oxygen levels. However, wind may be relevant in predicting DO levels in coastal basins with morphological and hydrodynamic characteristics significantly different from those of this study (e.g., greater water depth or different flushing regimes). For the application of a similar RF approach to such cases, an ad-hoc re-evaluation of the inclusion or exclusion of wind speed among predictors should be performed.

As far as the WRT is concerned, although some authors have highlighted a possible association between WRT and low DO values (e.g. Coffin et al., 2018), this study is the first to evaluate the predictive power of the parameter to assess oxygen deficiencies in a shallow water, partially enclosed lagoon environment. Results show that including WRT among the predictors enhances the TPR_{VL} of the RF-HD model from 80 % to 86 % for the Very low class (Fig. 5b–c). Even more relevantly, the performance of the RF-HD model increases from $TPR_L = 54$ % to $TPR_L = 67$ % for the class Low (2 mg/l < DO <4 mg/l). It is important to remark that the typical time scale of hypoxia occurrence in the lagoon (which often is sub-daily, as in Fig. 2) is much shorter than its WRT (i.e. >90 days in central, scarcely circulated, areas). This suggests that WRT can only be relevant, in association with the physical transport processes of DO across the lagoons' boundaries, in the areas closer to the inlets, where WRT is always limited and the probability of having very low DO concentrations is minimal. In the innermost areas of the lagoon, however, the WRT rather markedly characterizes the different responses of the two lagoon basins to the management of the pumping system at the inlets, with lower summer values in the Ponente basin and higher in the Levante basin. In these areas, therefore, the WRT parameter informs the model with a positional index, which in turn implicitly accounts for the different response of the lagoon, in terms of DO, to the environmental conditions observed in the two basins, further explaining the gain in the RF model accuracy observed when including the WRT.

5.2. Performance and limitations of the proposed modelling approach

The RF models showed satisfactory performance in classifying DO levels with contemporary predictors and output, for both versions based on measured quantities (RF-MEAS) and data derived from the hydrodynamic modelling of the lagoon (RF-HD), with a TPR_{VL} on the class Very low of 88 % and 86 %. It is worth noting that the TPR for the class Low was the lowest ($TPR_L = 69$ % for the RF-MEAS, 67 % for the RF-HD). This may be due to the reduced number of observations in that class. To prioritize the RF model's capability to detect hypoxia (i.e. DO levels in the Very low class), the SMOTE approach to correct class imbalance (*Section 3.3.1*) was applied to the Very low class only. Additionally, a further reason for the poorer performance in the Low class may be feature overlap: the RF algorithm may struggle to differentiate between the Low and the Middle DO classes due to overlapping feature values. Possible solutions to this issue, which are out of the scope of the present work, may include applying feature engineering techniques to create more discriminative features.

Starting from the idea that hypoxia is not an instantaneous process, but rather the result of the interaction of processes and environmental conditions in previous periods, time-lagged predictors were used to explore the performance of ML models in predicting DO in a lagoon for different forecast horizons. The same approach had been previously used by Politikos et al., 2021, for time lags of 2 to 20 days. The authors found similar performance of the models for the different time lags (with F1-score of 92 % and 93 % for the RF model with $N_{lag} = 2$ days and 20 days, respectively). In the present work, the persisting satisfactory performance of RF models in predicting DO is confirmed, with an F1-score on the class Very low of 86 %, for both the RF-MEAS and RF-HD models, with $N_{lag} = 10$ days.

RF model was trained with DO data from three measuring stations and it is designed to be potentially transferrable to any other point within the lagoon, allowing to extend the knowledge of DO conditions in space. Implicit in this approach is the strong assumption that the trained RF model's applicability transcends the specific training locations. This assumption is grounded in the hypothesis of substantial uniformity in those underlying processes governing DO dynamics which are not explicitly accounted for by the predictors of the RF model. These unaccounted factors include sediment characteristics (e.g. nutrient availability, mobilization, and resuspension potential), and vegetation (dominant species, density, and distribution), among others.

The possibility of applying the model to obtain spatially distributed knowledge of DO levels is supported by the example application presented in *Section 4.5*, where the model was shown to be able to quite accurately identify the most critical areas in terms of DO contents during selected hypoxic episodes in the summer of 2022. On the other hand, it is imperative to acknowledge the model's limitation in representing site-specific critical scenarios arising from localized phenomena that are independent of the considered predictive parameters. Examples of such phenomena include localized nutrient releases or the presence of algae species with DO dynamics differing from those observed during the model calibration period.

Additionally, it should be also emphasized that such a modelling approach is only deemed suitable for short-term applications, wherein the time intervals are sufficiently limited to reasonably assume that the conditions affecting the eutrophic nature of the lagoon, and not explicitly included in the model, have remained unchanged since its training. Among these conditions, the composition and activity of microbial and aquatic plant communities, as well as the overall influx of nutrients into the lagoon system (both from external sources and sediment release), are essential. As a relevant example, possible shifts in the water salinity levels occurring at a time scale longer than the 3-years period of the training dataset may decouple pH and DO from biological processes, due to changes in the biological communities' compositions. Such effects, absent in the training data, could not be captured and described by the RF model. Furthermore, the quality of sediment, concerning its chemical and physical attributes and its correlation with seagrass presence, is known to undergo significant evolution over time, further highlighting the inherent time-limited validity of the RF models presented in this study. Consequently, it is recommended to retrain the algorithm based on the most recent available data if significant alterations in the aforementioned conditions have occurred. Training the model on a longer dataset, extending the range of dynamic conditions observed in the data, could also be beneficial in allowing a longer-term applicability of the model.

6. Conclusions

This work investigated the effectiveness of predicting hypoxia in coastal lagoons through an integrated methodology involving hydrodynamic modelling, machine learning techniques (specifically, the Random Forest algorithm, RF), and in-situ measurements. The numerical model allows for the simulation of the hydrodynamics and heat exchange processes in the lagoon, providing also water temperature and salinity as an output. The proposed approach proved to be promising for the short-term prediction of DO levels with a high resolution in both time and space throughout the entire lagoon. Indeed, leveraging predictors derived from a hydrodynamic model allows for overcoming the intrinsic limitation of modelling approaches based on discrete in situ data measurements, i.e. the inability to capture the spatial heterogeneity of DO distributions.

The classification capability of DO levels was found to be similar for RF models trained on physical-chemical parameters collected at water quality monitoring stations in the lagoon (RF-MEAS models) or with predictors derived from the hydrodynamic model (RF-HD). An overall classification accuracy of around 91 % was found for both RF-MEAS and RF-HD models for the contemporary classification, with an F1 score for identifying the occurrence of hourly DO levels lower than 2 mg/l (often assumed as the threshold for severe hypoxia) higher than 86 %. The classification performance of the models remains satisfactory for a forecast horizon of up to 10 days.

Using the SHAP-values framework, the relative importance of the different factors was assessed and interpreted. Consistently with previous knowledge of the fundamental processes involved in DO dynamics in coastal lagoons, the most relevant predictors were found to be pH, water temperature, hour of the day, daytime duration and salinity for the RF-MEAS models. Relying on predictors derived from the hydrodynamic model, the most relevant features are the water temperature, salinity, and hour of the day.

The proposed modelling approach inherently assumes that any influential factors affecting DO, not explicitly included in the RF model, remain constant over the model's intended usage horizon, thereby restricting its applicability to short-term predictions. Nevertheless, the proposed approach, having identified a set of predictors strongly correlated with DO levels, is adaptable for retraining should there be significant changes in the boundary conditions. This flexibility allows the model to be updated and refined as new data are available. Moreover, the proposed modelling approach, with the identified set of predictors, could be applied to different water bodies with similar characteristics (e.g. water depth, flushing and water residence time), possibly after having trained a specific RF model based on data collected at the location of interest.

CRediT authorship contribution statement

Irene Simonetti: Writing – original draft, Validation, Software, Methodology, Investigation, Formal analysis, Conceptualization. **Claudio Lubello:** Writing – review & editing, Methodology, Conceptualization. **Lorenzo Cappietti:** Writing – review & editing, Methodology, Conceptualization.

Declaration of competing interest

The authors declare that they have no known competing financial interests or personal relationships that could have appeared to influence the work reported in this paper.

Data availability

Data will be made available on request.

Acknowledgments

The research was partially funded by the European Union-FSE-REACT-EU, PON Research and Innovation 2014–2020, D.M. 1062/2021, Contract Number 10-G-15057-1. This work received funding by the Tuscany Region Authority through the research agreement D.D. 20867 with date 24/11/2021.

Appendix A. Supplementary data

Supplementary data to this article can be found online at https://doi.org/10.1016/j.scitotenv.2024.175424.

References

Arfi, R., Guiral, D., Bouvy, M., 1993. Wind induced resuspension in a shallow tropical lagoon. Estuar. Coast. Shelf Sci. 36, 587–604. https://doi.org/10.1006/ecss.1993.1036.

Arrighi, C., 2023. Prediction of ecological status of surface water bodies with supervised machine learning classifiers. Sci. Total Environ. 857 (Part 3) https://doi.org/10.1016/j.scitotenv.2022.159655. ISSN 0048-9697.

Ascione Kenov, I., Garcia, A.C., Neves, R., 2012. Residence time of water in the Mondego estuary (Portugal). Estuar. Coast. Shelf Sci. 106, 13–22. https://doi.org/10.1016/j.ecss.2012.04.008.

Béjaoui, B., Armi, Z., Ottaviani, E., Barelli, E., Gargouri-Ellouz, E., Chérif, R., Turki, S., Solidoro, C., Aleya, L., 2016. Random Forest model and TRIX used in combination to assess and diagnose the trophic status of Bizerte Lagoon, southern Mediterranean. Ecol. Indic. 71, 293–301. https://doi.org/10.1016/j.ecolind.2016.07.010.

Béjaoui, B., Solidoro, C., Harzallah, A., Chevalier, C., Chapelle, A., Zaaboub, N., Aleya, L., 2017. 3D modeling of phytoplankton seasonal variation and nutrient budget in a southern Mediterranean Lagoon. Mar. Pollut. Bull. 114, 962–976. https://doi.org/10.1016/j.marpolbul.2016.11.001.

Béjaoui, B., Ottaviani, E., Barelli, E., Ziadi, B., Dhib, A., Lavoie, M., Gianluca, C., Turki, S., Solidoro, C., Aleya, L., 2018. Machine learning predictions of trophic status indicators and plankton dynamic in coastal lagoons. Ecol. Indic. 95, 765–774. https://doi.org/10.1016/j.ecolind.2018.08.041.

Boateng, I., Mitchell, S., Couceiro, F., Failler, P., 2020. An investigation into the impacts of climate change on anthropogenic polluted coastal lagoons in Ghana. Coast. Manag. 48, 601–622. https://doi.org/10.1080/08920753.2020.1803565.

Breiman, L., 2001. Random forests. Mach. Learn. 45, 5–32. https://doi.org/10.1023/A:1010933404324.

Breitburg, D., Levin, L.A., Oschlies, A., Grégoire, M., Chavez, F.P., Conley, D.J., Garçon, V., Gilbert, D., Gutiérrez, D., Isensee, K., Jacinto, G.S., Limburg, K.E., Montes, I., Naqvi, S.W.A., Pitcher, G.C., Rabalais, N.N., Roman, M.R., Rose, K.A., Seibel, B.A., Telszewski, M., Yasuhara, M., Zhang, J., 2018. Declining oxygen in the global ocean and coastal waters. Science 359, eaam7240. https://doi.org/10.1126/science.aam7240.

Bui, D.T., Khosravi, K., Tiefenbacher, J., Nguyen, H., Kazakis, N., 2020. Improving prediction of water quality indices using novel hybrid machine-learning algorithms. Sci. Total Environ. 721, 137612 https://doi.org/10.1016/j.scitotenv.2020.137612.

Caballero-Alfonso, A.M., Carstensen, J., Conley, D.J., 2015. Biogeochemical and environmental drivers of coastal hypoxia. J. Mar. Syst. 141, 190–199. https://doi.org/10.1016/j.jmarsys.2014.04.008.

Chawla, N.V., Bowyer, K.W., Hall, L.O., Kegelmeyer, W.P., 2002. SMOTE: synthetic minority over-sampling technique. J Artif Intell Res 16, 321–357. https://doi.org/10.1613/jair.953.

Cioffi, F., Di Eugenio, A., Gallerano, F., 1995. A new representation of anoxic crises in hypertrophic lagoons. Appl. Math. Model. 19 (11), 685–695. https://doi.org/10.1016/0307-904X(95)00075-U. ISSN 0307-904X.

Clementi, E., Aydogdu, A., Goglio, A.C., Pistoia, J., Escudier, R., Drudi, M., Grandi, A., Mariani, A., Lyubartsev, V., Lecci, R., Cretí, S., Coppini, G., Masina, S., Pinardi, N., 2021. Mediterranean Sea Physical Analysis and Forecast (CMEMS MED-Currents, EAS6 system): MEDSEA_ANALYSISFORECAST_PHY_006_013 doi:10.25423/CMCC/MEDSEA_ANALYSISFORECAST_PHY_006_013_EAS6.

Coffin, M.R.S., Courtenay, S.C., Pater, C.C., van den Heuvel, M.R., 2018. An empirical model using dissolved oxygen as an indicator for eutrophication at a regional scale. Mar. Pollut. Bull. 133, 261–270. https://doi.org/10.1016/j.marpolbul.2018.05.041.

Cucco, A., Umgiesser, G., 2006. Modeling the Venice Lagoon residence time. Ecol. Model. 193, 34–51. https://doi.org/10.1016/j.ecolmodel.2005.07.043.

D'Avanzo, C., Kremer, J., Wainright, S., 1996. Ecosystem production and respiration in response to eutrophication in shallow temperate estuaries. Mar. Ecol. Prog. Ser. 141, 263–274. https://doi.org/10.3354/meps141263.

Diaz, R.J., Rosenberg, R., 2008. Spreading dead zones and consequences for marine ecosystems. Science 321, 926–929. https://doi.org/10.1126/science.1156401.

Duarte, C.M., Hendriks, I.E., Moore, T.S., Olsen, Y.S., Steckbauer, A., Ramajo, L., Carstensen, J., Trotter, J.A., McCulloch, M., 2013. Is ocean acidification an open-ocean syndrome? Understanding anthropogenic impacts on seawater pH. Estuar. Coasts 36, 221–236. https://doi.org/10.1007/s12237-013-9594-3.

Elreedy, D., Atiya, A.F., 2019. A comprehensive analysis of synthetic minority oversampling technique (SMOTE) for handling class imbalance. Inform. Sci. 505, 32–64. https://doi.org/10.1016/j.ins.2019.07.070.

Garcia, H.E., Gordon, L.I., 1992. Oxygen solubility in seawater: better fitting equations. Limnol. Oceanogr. 37, 1307–1312. https://doi.org/10.4319/lo.1992.37.6.1307.

Gobler, C.J., Baumann, H., 2016. Hypoxia and acidification in ocean ecosystems: coupled dynamics and effects on marine life. Biol. Lett. 12, 20150976. https://doi.org/10.1098/rsbl.2015.0976.

Gogoi, P., Das, S.K., Jana, C., Das, B.K., Saha, A., Ramteke, K., Jaiswar, A.K., Samanta, S., Roshith, C.M., 2024. Assessing the trophic status of a tropical microtidal estuary applying TRIX and Random Forest – a combined approach. Mar. Pollut. Bull. 200, 116126 https://doi.org/10.1016/j.marpolbul.2024.116126.

Hadid, N.B., Goyet, C., Chaar, H., Maiz, N.B., Guglielmi, V., Shili, A., 2021. Machine learning modeling techniques for forecasting the trophic level in a restored South Mediterranean Lagoon using chlorophyll-a. Wetlands 41, 111. https://doi.org/10.1007/s13157-021-01479-6.

Hastie, T., Tibshirani, R., Friedman, J.H., 2009. The Elements of Statistical Learning: Data Mining, Inference, and Prediction, 2nd ed. ed. Springer series in statistics, Springer, New York, NY.

Hull, V., Parrella, L., Falcucci, M., 2008. Modelling dissolved oxygen dynamics in coastal lagoons. Ecol. Model. 211, 468–480. https://doi.org/10.1016/j.ecolmodel.2007.09.023.

Larsen, S.B., 2024. Synthetic Minority Over-sampling Technique (SMOTE). https://github.com/dkbsl/matlab_smote/releases/tag/1.0.

Lenzi, M., Palmieri, R., Porrello, S., 2003. Restoration of the eutrophic Orbetello lagoon (Tyrrhenian Sea, Italy): water quality management. Mar. Pollut. Bull. 46, 1540–1548. https://doi.org/10.1016/S0025-326X(03)00315-1.

Lenzi, M., Gennaro, P., Mercatali, I., Persia, E., Solari, D., Porrello, S., 2013. Physico-chemical and nutrient variable stratifications in the water column and in macroalgal thalli as a result of high biomass mats in a non-tidal shallow-water lagoon. Mar. Pollut. Bull. 75, 98–104. https://doi.org/10.1016/j.marpolbul.2013.07.057.

Leporatti Persiano, M., 2022. Nota n.4_2022, Laguna di Orbetello, Resoconto stagione estiva e analisi della situazione attuale – Settembre 2022, CUP: D39J21020740002. Technical Note for Tuscany Region authority (in Italian).

Liang, W., Liu, T., Wang, Y., Jiao, J.J., Gan, J., He, D., 2023. Spatiotemporal-aware machine learning approaches for dissolved oxygen prediction in coastal waters. Sci. Total Environ. 905, 167138 https://doi.org/10.1016/j.scitotenv.2023.167138.

López, V., Fernández, A., García, S., Palade, V., Herrera, F., 2013. An insight into classification with imbalanced data: empirical results and current trends on using data intrinsic characteristics. Inform. Sci. 250, 113–141. https://doi.org/10.1016/j.ins.2013.07.007.

Lundberg, S., Lee, S.-I., 2017. A Unified Approach to Interpreting Model Predictions. https://doi.org/10.48550/ARXIV.1705.07874.

Lundberg, S.M., Erion, G.G., Lee, S.-I., 2019. Consistent Individualized Feature Attribution for Tree Ensembles.

Lundberg, S.M., Erion, G., Chen, H., DeGrave, A., Prutkin, J.M., Nair, B., Katz, R., Himmelfarb, J., Bansal, N., Lee, S.-I., 2020. From local explanations to global understanding with explainable AI for trees. Nat. Mach. Intell. 2, 56–67. https://doi.org/10.1038/s42256-019-0138-9.

Mauro Lenzi, L., Gennaro, P., Rubegni, F., 2016. Wind mitigating action on effects of eutrophication in coastal eutrophic water bodies. Wind mitigating action eff. eutrophication coast. In: Eutrophic Water Bodies, pp. 14–20. https://doi.org/10.19070/2577-4395-160004.

Melzner, F., Thomsen, J., Koeve, W., Oschlies, A., Gutowska, M.A., Bange, H.W., Hansen, H.P., Körtzinger, A., 2013. Future ocean acidification will be amplified by hypoxia in coastal habitats. Mar. Biol. 160, 1875–1888. https://doi.org/10.1007/s00227-012-1954-1.

Newton, A., Icely, J., Cristina, S., Brito, A., Cardoso, A.C., Colijn, F., Riva, S.D., Gertz, F., Hansen, J.W., Holmer, M., Ivanova, K., Leppäkoski, E., Canu, D.M., Mocenni, C., Mudge, S., Murray, N., Pejrup, M., Razinkovas, A., Reizopoulou, S., Pérez-Ruzafa, A., Schernewski, G., Schubert, H., Carr, L., Solidoro, C., PierluigiViaroli, Zaldívar, J.-M., 2014. An overview of ecological status, vulnerability and future perspectives of European large shallow, semi-enclosed coastal systems, lagoons and transitional waters. Estuar. Coast. Shelf Sci. 140, 95–122. https://doi.org/10.1016/j.ecss.2013.05.023.

Politikos, D.V., Petasis, G., Katselis, G., 2021. Interpretable machine learning to forecast hypoxia in a lagoon. Ecol. Inform. 66, 101480 https://doi.org/10.1016/j.ecoinf.2021.101480.

Pourzangbar, A., Jalali, M., Brocchini, M., 2023. Machine learning application in modelling marine and coastal phenomena: a critical review. Front. Environ. Eng. 2, 1235557 https://doi.org/10.3389/fenve.2023.1235557.

Ro, K.S., Hunt, P.G., Poach, M.E., 2007. Wind-driven surficial oxygen transfer. Crit. Rev. Environ. Sci. Technol. 37, 539–563. https://doi.org/10.1080/10643380601174749.

Rodrigues, M., Rosa, A., Cravo, A., Jacob, J., Fortunato, A.B., 2021. Effects of climate change and anthropogenic pressures in the water quality of a coastal lagoon (Ria Formosa, Portugal). Sci. Total Environ. 780, 146311 https://doi.org/10.1016/j.scitotenv.2021.146311.

Rodríguez-Gallego, L., Achkar, M., Defeo, O., Vidal, L., Meerhoff, E., Conde, D., 2017. Effects of land use changes on eutrophication indicators in five coastal lagoons of the Southwestern Atlantic Ocean. Estuar. Coast. Shelf Sci. 188, 116–126. https://doi.org/10.1016/j.ecss.2017.02.010.

Roman, M.R., Brandt, S.B., Houde, E.D., Pierson, J.J., 2019. Interactive effects of hypoxia and temperature on coastal pelagic zooplankton and fish. Front. Mar. Sci. 6, 139. https://doi.org/10.3389/fmars.2019.00139.

Rossman, L.A., Huber, W.C., 2016. Storm Water Management Model Reference Manual Volume I – Hydrology (Revised).

Rubbens, P., Brodie, S., Cordier, T., Destro Barcellos, D., Devos, P., Fernandes-Salvador, J.A., Fincham, J.I., Gomes, A., Handegard, N.O., Howell, K., Jamet, C., Kartveit, K.H., Moustahfid, H., Parcerisas, C., Politikos, D., Sauzède, R., Sokolova, M., Uusitalo, L., Van den Bulcke, L., van Helmond, A.T.M., Watson, J.T., Welch, H., Beltran-Perez, O., Chaffron, S., Greenberg, D.S., Kühn, B., Kiko, R., Lo, M., Lopes, R.M., Möller, K.O., Michaels, W., Pala, A., Romagnan, J.-B., Schuchert, P., Seydi, V., Villasante, S., Malde, K., Irisson, J.-O., 2023. Machine learning in marine ecology: an overview of techniques and applications. ICES J. Mar. Sci. 80, 1829–1853. https://doi.org/10.1093/icesjms/fsad100.

Seiler, L.M.N., Fernandes, E.H.L., Siegle, E., 2020. Effect of wind and river discharge on water quality indicators of a coastal lagoon. Reg. Stud. Mar. Sci. 40, 101513 https://doi.org/10.1016/j.rsma.2020.101513.

Shumka, S., Nagahama, Y., Hoxha, S., Asano, K., 2023. Overfishing and recent risk for collapse of fishery in coastal Mediterranean lagoon ecosystem (Karavasta lagoon, southeastern Adriatic sea). Fish. Aquat. Sci. 26, 294–303. https://doi.org/10.47853/FAS.2023.e25.

Simonetti, I., Cappietti, L., 2022. Influence of inlets morphology and forcing mechanisms on water exchange between coastal basins and the sea: a hindcast study for a Mediterranean Lagoon. J. Mar. Sci. Eng. 10, 1929. https://doi.org/10.3390/jmse10121929.

Soria, J., Pérez, R., Sòria-Pepinyà, X., 2022. Mediterranean coastal lagoons review: sites to visit before disappearance. J. Mar. Sci. Eng. 10, 347. https://doi.org/10.3390/jmse10030347.

Tyler, R.M., Brady, D.C., Targett, T.E., 2009. Temporal and spatial dynamics of diel-cycling hypoxia in estuarine tributaries. Estuaries Coasts 32, 123–145. https://doi.org/10.1007/s12237-008-9108-x.

Tyralis, H., Papacharalampous, G., Langousis, A., 2019. A brief review of random forests for water scientists and practitioners and their recent history in water resources. Water 11, 910. https://doi.org/10.3390/w11050910.

Valera, M., Walter, R.K., Bailey, B.A., Castillo, J.E., 2020. Machine learning based predictions of dissolved oxygen in a small coastal embayment. J. Mar. Sci. Eng. 8, 1007. https://doi.org/10.3390/jmse8121007.

Vaquer-Sunyer, R., Duarte, C.M., 2008. Thresholds of hypoxia for marine biodiversity. Proc. Natl. Acad. Sci. 105, 15452–15457. https://doi.org/10.1073/pnas.0803833105.

Wang, S.S.-C., Qian, Y., Leung, L.R., Zhang, Y., 2021. Identifying key drivers of wildfires in the contiguous US using machine learning and game theory interpretation. Earths Future 9, e2020EF001910. https://doi.org/10.1029/2020EF001910.

Zannella, A., Simonetti, I., Lubello, C., Cappietti, L., 2024. Hydrodynamics, transport time scales and water temperature dynamics in heavily anthropized eutrophic coastal lagoons, submitted for publication. available at: https://papers.ssrn.com/sol3/papers.cfm?abstract_id=4823310.

Zennaro, F., Furlan, E., Canu, D., Aveytua Alcazar, L., Rosati, G., Solidoro, C., Aslan, S., Critto, A., 2023. Venice lagoon chlorophyll-a evaluation under climate change conditions: a hybrid water quality machine learning and biogeochemical-based framework. Ecol. Indic. 157, 111245 https://doi.org/10.1016/j.ecolind.2023.111245.

Ziegler, A., König, I.R., 2014. Mining data with random forests: current options for real-world applications. WIREs Data Min. Knowl. Discov. 4, 55–63. https://doi.org/10.1002/widm.1114.